AIP Journal of Applied Physics

Calculating the responsivity of a resonant-cavity-enhanced Si 1 − x Ge x / Si multiple quantum well photodetector

Mukul K. Das and N. R. Das

Citation: Journal of Applied Physics **105**, 093118 (2009); doi: 10.1063/1.3117519
View online: http://dx.doi.org/10.1063/1.3117519
View Table of Contents: http://scitation.aip.org/content/aip/journal/jap/105/9?ver=pdfcov
Published by the AIP Publishing

Calculating the responsivity of a resonant-cavity-enhanced $Si_{1-x}Ge_x/Si$ multiple quantum well photodetector

Mukul K. Das[1,a)] and N. R. Das[2,b)]
[1]*A. K. Choudhury School of Information Technology, University of Calcutta, 92 Acharya P. C. Road, Kolkata—700009, India*
[2]*Institute of Radio Physics and Electronics, University of Calcutta, 92 Acharya P. C. Road, Kolkata—700009, India*

(Received 4 August 2008; accepted 20 March 2009; published online 14 May 2009)

In this paper, the responsivity of a resonant-cavity-enhanced SiGe/Si multiple quantum well photodetector has been theoretically investigated. The present model considers the effects of material parameters of $Si_{1-x}Ge_x$ and recombination of carriers confined by the potential barriers at the heterointerfaces of $Si_{1-x}Ge_x/Si$ quantum wells on the detector responsivity for different Ge-contents (x). The effect of electric field due to applied bias on the emission of confined carriers from quantized subbands has also been included in the analysis. Results show that though high Ge-content is required to enhance the responsivity of the SiGe/Si photodetector for long-haul communication (at 1.3 and 1.55 μm), the confinement of holes at the heterointerfaces may be significant to affect the responsivity adversely. Studies at 1.3 and 1.55 μm also show that the responsivity of the photodetector for a particular Ge-content in the active layer can be increased by suitable choice of well parameters and applied bias. © *2009 American Institute of Physics*. [DOI: 10.1063/1.3117519]

I. INTRODUCTION

Photodetectors play key role in the high performance of a multigigabit optical communication system.[1,2] III–V-based photodetectors have already shown excellent performance in such applications. Recently, Si-based photodetectors have attracted a lot of interest among researchers around the world mainly due to its low cost, CMOS compatibility, and high integrability.[3–8] Performance of the Si photodetectors, however, is not satisfactory for long-haul optical communication due to the weak absorption characteristics of Si at long wavelengths such as 1.3 and 1.55 μm. The incorporation of a small amount of Ge into Si helps in the shifting of the absorption peak toward longer wavelengths. Significant absorption can be achieved in a SiGe photodiode at longer wavelengths by increasing the Ge-content in the SiGe alloy. However, because of lattice mismatch between Ge and Si, it has been demonstrated that the SiGe alloy can be grown on a Si substrate (i.e., lattice mismatch is tolerable) if the thickness of the SiGe layer is kept below a critical value.[9] This critical value decreases with the increase in the Ge-content and, so, for higher wavelength applications, the SiGe layer is constrained to be thinner. Although the thin absorption layer is suitable for high-speed operation of a transit-time limited photodetector, it reduces the quantum efficiency and, hence, responsivity of the detector. This thin active layer can be placed inside a resonant cavity[10,11] and due to multiple reflections inside the cavity the optical field increases resulting in the increase in responsivity of the photodetector. When the layer is very thin, such as a quantum well (QW), the resonant cavity alone is not sufficient to increase the responsivity significantly. The use of multiple QWs as the absorption layer helps in this case. Thus, enhanced responsivity can be obtained by placing a $Si_{1-x}Ge_x$ multiple quantum well (MQW) photodetector structure inside a resonant cavity. The presence of heterojunction in such structures affects the responsivity and, so, appropriate modeling is required considering this effect to predict the best possible design of the photodetector for high responsivity. To the knowledge of the authors, this important aspect has not been considered earlier on the modeling of the responsivity of photodetector.

In this paper, we have made a detailed study to calculate the responsivity of a resonant cavity enhanced (RCE) $Si_{1-x}Ge_x/Si$ MQW photodetector for different Ge-contents considering the effect of confinement of carriers in the potential trap at the heterointerfaces. The remaining sections of this paper are organized as follows. A theoretical background is given in Sec. II. The results from the computation are discussed in Sec. III. Finally, in Sec. IV, a conclusion is given.

II. THEORETICAL BACKGROUND

In this section, Ge-content dependent material properties of the active SiGe (alloy) layer and carrier confinement at the heterointerface of a SiGe/Si QW structure are described. Then, considering the above effects in association with the optical field distributions within the active layer in a resonant cavity, the responsivity of a RCE SiGe/Si MQW photodetector is calculated.

A. Material considerations

Material properties of a Ge-incorporated Si layer change depending on the Ge-content. We have used Vegards' law to

a)Present Address: Department of Electron. and Instrument., Indian School of Mines University, Dhanbad, India.
b)Tel.: +91 33 2350 9115. FAX: +91 33 2351 5828. Electronic addresses: mukulkdas@ieee.org and nrd@ieee.org.

TABLE I. Material parameters of SiGe for different Ge-content (x) (ΔE_c=0.03 eV assumed).

	$\alpha_{SiGe}(m^{-1})$ (for d_w=20 nm)						$\mu_{SiGe}(m^2/V\ s)$		$v_{sat,SiGe}(m/s)$			
x	λ=0.69 μm	λ=0.85 μm	λ=1.0 μm	λ=1.3 μm	λ=1.55 μm	$\varepsilon_{r,SiGe}$	Electron	Hole	Electron	Hole	ΔE_g (eV)	ΔE_v (eV)
0.1	3.2×10^6	7.9×10^5	9.9×10^4	0	0	12.31	0.174	0.0595	8.9×10^4	4.4×10^4	0.08	0.05
0.2	4.0×10^6	1.3×10^6	3.0×10^5	0.556	0	12.72	0.198	0.0740	8.8×10^4	4.8×10^4	0.17	0.14
0.3	5.1×10^6	1.9×10^6	6.2×10^5	7.9×10^3	0	13.13	0.222	0.0885	8.7×10^4	5.2×10^4	0.26	0.23
0.4	6.9×10^6	2.8×10^6	1.1×10^6	5.8×10^4	0	13.54	0.246	0.103	8.6×10^4	5.6×10^4	0.32	0.29
0.5	9.2×10^6	4.0×10^6	1.8×10^6	2.3×10^5	5.3×10^3	13.95	0.27	0.118	8.5×10^4	6.0×10^4	0.39	0.36

approximate some material parameters of the $Si_{1-x}Ge_x$ alloy for different Ge-content (x). For example, relative permittivity of $Si_{1-x}Ge_x$, $\varepsilon_{r,SiGe}$ is given by

$$\varepsilon_{r,SiGe} = \varepsilon_{r,Si} \times (1-x) + \varepsilon_{r,Ge} \times x \tag{1}$$

where $\varepsilon_{r,Si}$ and $\varepsilon_{r,Ge}$ are the relative permittivities of Si and Ge, respectively. Similarly, mobility and saturation velocity are also calculated. Numerical values of some material parameters for different x are given in Table I.

The absorption coefficient[12] of SiGe alloy (α_{SiGe}) is calculated using the relation

$$\alpha_{SiGe} = Z \times \left[\frac{(h\nu - E_{g,SiGe} - k\theta)^2}{1-\exp(-\theta/T)} + \frac{(h\nu - E_{g,SiGe} + k\theta)^2}{\exp(-\theta/T)-1} \right], \tag{2}$$

where ν is the frequency of light wave, k is Boltzmann constant, θ is the average phonon equivalent temperature, h is the Plank's constant, T is the absolute temperature, $E_{g,SiGe}$ is the band gap of SiGe alloy, and Z is a substantially temperature-independent proportionality factor. The two terms within the bracket on the right hand side of Eq. (2) appear due to phonon creation ($-k\theta$) and phonon annihilation ($+k\theta$) to assist optical absorption in an indirect band-gap semiconductor. The band gap and the phonon equivalent temperature of SiGe alloy depend on the Ge-content.[12,13]

B. Carrier confinement at heterointerface

Let us consider a typical layer structure of RCE $Si_{1-x}Ge_x$/Si MQW photodetector shown in Fig. 1(a). Bragg reflectors serve as the mirrors of the resonant cavity. When light of suitable wavelength is incident on the active layer (SiGe), electron-hole pairs (EHPs) are generated. These photogenerated electrons and holes move in opposite directions giving rise to photocurrent. The photogenerated carriers on their transit get confined at the heterointerfaces due to potential barrier, viz., holes are confined at the P–Si/i-SiGe interface due to band offset in the valence band, and electrons are confined at the i-SiGe/N–Si interface due to offset in the conduction band. To illustrate this, the carrier confinement in a P–Si/i-SiGe/N–Si structure is shown by its band diagram in Fig. 1(b). The carriers confined at the interface are emitted by a slow thermionic emission process over the potential barrier and, so, take a long time to reach the metal contacts. The confinement of the carriers for a long time at the heterointerface results in the loss of carriers by recombination. This causes the overall photocurrent (hence, responsivity) to decrease. To calculate the effect of carrier confinement at the heterointerface, we need to know the rate of thermionic emission of carriers. The rate of thermionic emission of holes (γ_{ho}) from the potential trap at the heterointerface in valence band can be obtained from

$$\gamma_{ho} = B\exp(-e_{vd}/kT), \tag{3}$$

where e_{vd} is the effective potential barrier for holes at the heterointerface and B is a constant.[14] Similarly, the rate of emission of electrons from the potential trap at the heterointerface can be calculated. Thus, the calculation of emission rate requires the knowledge of the effective barrier heights for electrons and holes at the interfaces. These barrier heights, however, depend on the offsets ΔE_c and ΔE_v in the respective bands and the applied reverse bias. The values of these band offsets for different Ge-contents are derived using the interpolation of the available experimental data.[13]

The photodetector in our consideration consists of MQWs as shown in Fig. 2(a). In a QW, the energy levels are quantized and the ground state is lifted up. So, the effective barrier height is reduced as shown in Fig. 2(b) for no bias

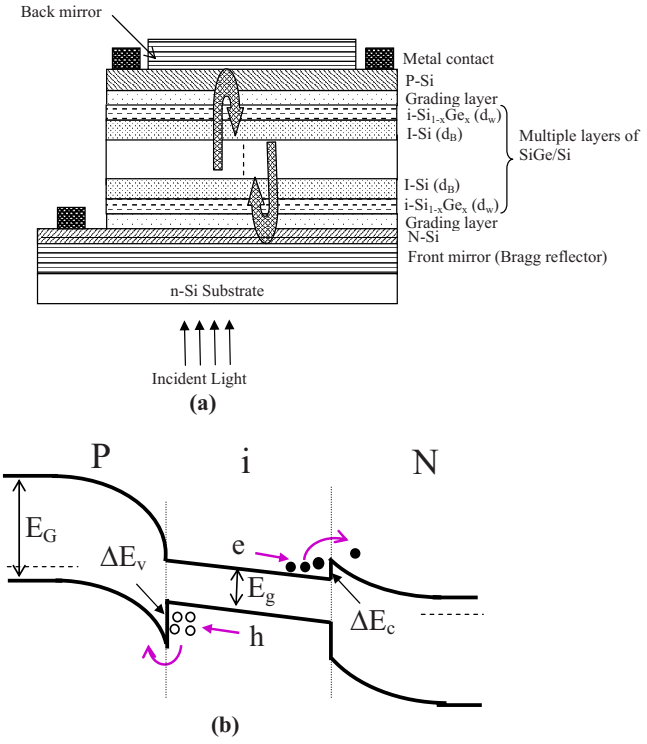

FIG. 1. (Color online) (a) Schematic structure of a RCE SiGe/Si MQW photodetector. (b) Band diagram of a P–Si/i-SiGe/N–Si structure showing carrier confinement at heterointerfaces.

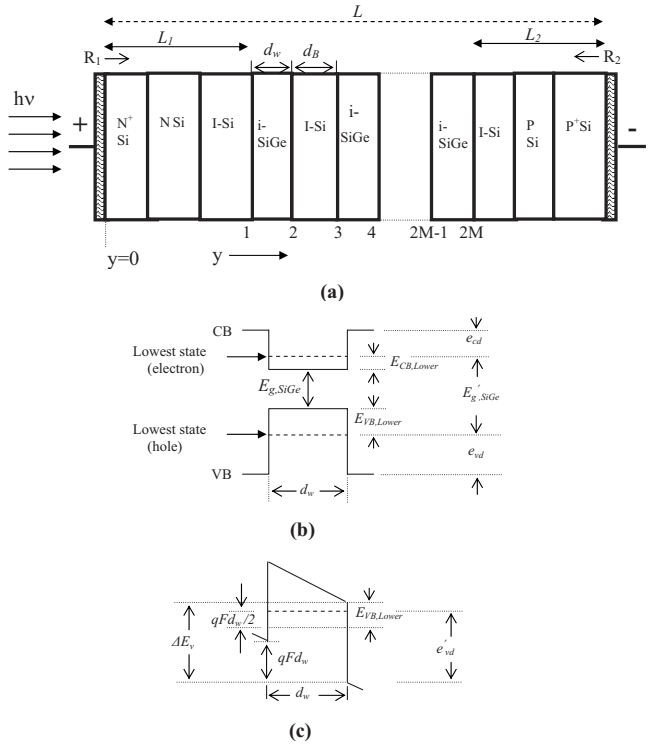

FIG. 2. (a) Lateral view of a RCE SiGe/Si MQW photodetector. Numbers $(1,2,\ldots,2M)$ at the bottom of the diagram indicate the positions of heterointerfaces. Electrons are confined at the odd-numbered interfaces while holes are confined at the even-numbered interfaces. (b) Energy band diagram of a single well at no bias. (c) Valence-band diagram of a single well under bias.

condition. Here, we have assumed that only one energy state is present in the well. In order to calculate the effective barrier height (e'_{vd}) for the confined holes in a biased QW, we consider the valence band diagram of a single well as shown in Fig. 2(c). So, we may write

$$e'_{vd} = \Delta E_v - E_{\mathrm{VB,Lower}} - qFd_w/2, \tag{4}$$

where d_w is the well thickness, F is the electric field in the well due to the applied bias, and $E_{\mathrm{VB,Lower}}$ is the position of the lowest energy states in the QW with respect to the top of the valence band and is given by

$$E_{\mathrm{VB,Lower}} = \frac{\hbar^2}{2m_h^*}\left(\frac{\pi}{d_w}\right)^2, \tag{5}$$

where m_h^* is the effective mass of holes. So, e_{vd} in Eq. (3) is replaced by e'_{vd} to calculate the emission rate of holes from a QW. Similarly, the emission rate of electrons from a QW can be calculated. The effect of such confinement of holes and electrons at multiple heterointerfaces is considered to calculate the photocurrent and, hence, the responsivity of a MQW photodetector as discussed in Sec. II C. It may be mentioned here that for the estimation of α_{SiGe} in case of a QW structure, $E_{g,\mathrm{SiGe}}$ in Eq. (2) should be replaced by $E'_{g,\mathrm{SiGe}}$, the sum of $E_{g,\mathrm{SiGe}}$, $|E_{\mathrm{VB,Lower}}|$, and $|E_{\mathrm{CB,Lower}}|$ as shown in Fig. 2(b).

C. Responsivity calculation

The responsivity $(\Re)$ of a photodetector is defined as the ratio of the dc photocurrent to the incident optical power,

$$\Re = \frac{JA}{P_i}, \tag{6}$$

where J is the photocurrent density, A is effective area of the detector, and P_i is the incident optical power. So, to obtain responsivity, we first calculate the photocurrent density in the photodetector.

Let us consider the case of holes first. As shown in the lateral schematic structure, Fig. 2(a), the coordinate y is directed from N to P, direction of flow of holes. The active layer is assumed intrinsic, so the field is constant in this region and the carriers move with constant velocity. The continuity equation for holes can then be written in a simplified form as

$$\frac{\partial p(y,t)}{\partial t} + v_h\frac{\partial p(y,t)}{\partial y} = g(y,t) - \frac{(p-p_0)}{\tau_h}, \tag{7}$$

where p_0 is equilibrium hole density, τ_h is the recombination time of holes, v_h is the velocity of holes, and $g(y,t)$ is the EHP generation rate. The electric field is uniform in the intrinsic layer (SiGe) and, so, the velocity v_h is constant throughout this layer for a particular bias. In addition, if the layer is very thin, the field may be high enough even at low reverse bias (plus contact potential); so saturation velocity may also be assumed. The expression for saturation velocity of holes in $Si_{1-x}Ge_x$ layer has been obtained knowing the saturation velocity of holes in Si and Ge, and then using the Vegard's law [similar to Eq. (1)]. Some values of saturation velocities in SiGe are given in Table I. In our computation, we have used field dependent velocity for very low bias. Photogeneration occurs in active regions (here, QWs) only. To indicate the generation rate in the rth QW, $g(y,t)$ will be replaced by $g_r(y,t)$.

Now, assuming low-level illumination and denoting the current density due to moving holes by j_{hm}, the rate equations for holes in the valence band can be written as,

$$dp_\tau/dt = j_{\mathrm{hm}}/q - (\gamma_{\mathrm{ho}} + \gamma_{\mathrm{rh}})p_\tau, \tag{8}$$

where γ_{rh} is the recombination rate for holes $(\sim 1/\tau_h)$ and p_τ represents the holes confined per unit area at the heterointerface. Similar equations can be written for electrons also. Now, the continuity and rate equations [as in Eqs. (7) and (8)] can be solved under dc condition to get the emitted carrier density. To solve Eq. (7), we have considered the position dependent generation rate due to the incident light impulse. For the MQW photodetector structure shown in Fig. 2(a), the generation rate in the rth QW can be calculated as

$$g_r(y,t) = \frac{P_i\alpha_{\mathrm{SiGe}}(1-R_1)e^{-\alpha_{\mathrm{SiGe}}Md_w}[e^{\alpha_{\mathrm{SiGe}}\{L_1+(r-1)d_B+Md_w-y\}} + R_2e^{-\alpha_{\mathrm{SiGe}}\{L_1+(r-1)d_B+Md_w-y\}}]}{Ah\nu[1-2\sqrt{R_1R_2}e^{-\alpha_{\mathrm{SiGe}}Md_w}\cos(2\beta L+\varphi_1+\varphi_2)+R_1R_2e^{-2\alpha_{\mathrm{SiGe}}Md_w}]}\delta(t), \tag{9}$$

where $R_1(R_2)$ and $\varphi_1(\varphi_2)$ are the reflectivity and phase shift, respectively, due to penetration of light at the front (back) mirror, $\delta(t)$ is the unit impulse (light) function of time, L is the length of the cavity, d_B is the barrier thickness, L_1 is the distance of the nearest well from the front mirror, M is the number of wells, and β is the propagation constant. The above equation shows that $g_r(y,t)$ passes through some maxima when $2\beta L+\varphi_1+\varphi_2=2m\pi$ $(m=1,2,3,\ldots,)$, other parameters remaining unchanged. In the present analysis/computation, the length of the cavity (L) is so assumed that this condition is satisfied.

The continuity equations are solved for each layer with appropriate boundary conditions. The carrier distribution in a layer depends on the carriers coming from the previous layer after surviving loss at the intermediate heterointerfaces. After a detailed calculation, the dc current densities due to photogenerated holes (J_p) and electrons (J_n) in the structure can be written, respectively, as

$$J_p = F1 \times \sum_{r=1}^{M} \left[\frac{e^{\alpha_{\mathrm{SiGe}}(M-r)d_w}}{\frac{1}{\tau_h v_h} - \alpha_{\mathrm{SiGe}}} \left\{ \frac{e^{\alpha_{\mathrm{SiGe}}d_w} - 1}{\alpha_{\mathrm{SiGe}}} - \frac{e^{\alpha_{\mathrm{SiGe}}d_w}(1 - e^{-d_w/v_h\tau_h})}{1/v_h\tau_h} \right\} + \frac{R_2 e^{-\alpha_{\mathrm{SiGe}}(M-r)d_w}}{\frac{1}{v_h\tau_h} + \alpha_{\mathrm{SiGe}}} \left\{ \frac{1 - e^{-\alpha_{\mathrm{SiGe}}d_w}}{\alpha_{\mathrm{SiGe}}} - \frac{e^{-\alpha_{\mathrm{SiGe}}d_w}(1 - e^{-d_w/v_h\tau_h})}{1/v_h\tau_h} \right\} + \sum_{i=1}^{r-1} e^{-(i-1)d_w/v_h\tau_h} \left\{ \frac{e^{\alpha_{\mathrm{SiGe}}(M-r+i)d_w}(1 - e^{\alpha_{\mathrm{SiGe}}d_w}e^{-d_w/v_h\tau_h})}{\frac{1}{v_h\tau_h} - \alpha_{\mathrm{SiGe}}} + \frac{R_2 e^{-\alpha_{\mathrm{SiGe}}(M-r+i)d_w}}{\frac{1}{v_h\tau_h} + \alpha_{\mathrm{SiGe}}}(1 - e^{-\alpha_{\mathrm{SiGe}}d_w}e^{-d_w/v_h\tau_h}) \right\} \times f_h^i \times \frac{1 - e^{-d_w/v_h\tau_h}}{1/v_h\tau_h} \right] \times f_h^r \tag{10}$$

$$J_n = F1 \times \sum_{r=1}^{M} \left[\frac{e^{\alpha_{\mathrm{SiGe}}(M-r)d_w}}{\frac{1}{\tau_e v_e} + \alpha_{\mathrm{SiGe}}} \left\{ \frac{e^{\alpha_{\mathrm{SiGe}}d_w} - 1}{\alpha_{\mathrm{SiGe}}} - \frac{(1 - e^{-d_w/v_e\tau_e})}{1/v_e\tau_e} \right\} + \frac{R_2 e^{-\alpha_{\mathrm{SiGe}}(M-r)d_w}}{\frac{1}{v_e\tau_e} - \alpha_{\mathrm{SiGe}}} \left\{ \frac{1 - e^{-\alpha_{\mathrm{SiGe}}d_w}}{\alpha_{\mathrm{SiGe}}} - \frac{(1 - e^{-d_w/v_e\tau_e})}{1/v_e\tau_e} \right\} + \sum_{i=1}^{M-r} e^{-(i-1)d_w/v_e\tau_e} \left\{ \frac{e^{\alpha_{\mathrm{SiGe}}(M-r-i)d_w}(e^{\alpha_{\mathrm{SiGe}}d_w} - e^{-d_w/v_e\tau_e})}{\frac{1}{v_e\tau_e} + \alpha_{\mathrm{SiGe}}} + \frac{R_2 e^{-\alpha_{\mathrm{SiGe}}(M-r-i)d_w}}{\frac{1}{v_e\tau_e} - \alpha_{\mathrm{SiGe}}}(e^{-\alpha_{\mathrm{SiGe}}d_w} - e^{-d_w/v_e\tau_e}) \right\} \times f_e^i \times \frac{1 - e^{-d_w/v_e\tau_e}}{1/v_e\tau_e} \right] \times f_e^{M-r+1} \tag{11}$$

where $f_h=\gamma_{h0}/(\gamma_{h0}+\gamma_{rh})$ and $f_e=\gamma_{e0}/(\gamma_{e0}+\gamma_{re})$, γ_{re} being the recombination rate of electrons, and $F1$ is a factor given by

$$F1 = \frac{q\alpha_{\mathrm{SiGe}}}{Md_w}\frac{P_i}{Ah\nu} \times \frac{(1-R_1)e^{-\alpha_{\mathrm{SiGe}}Md_w}}{[1 - 2\sqrt{R_1R_2}e^{-\alpha_{\mathrm{SiGe}}Md_w}\cos(2\beta L + \varphi_1 + \varphi_2) + R_1R_2e^{-2\alpha_{\mathrm{SiGe}}Md_w}]}. \tag{12}$$

The summation signs in Eqs. (10) and (11) take into account the effect of all QW layers. Terms with and without R_2 appear due to the corresponding terms in the expression for $g_r(y,t)$. The total current density (J) is given by sum of the hole and electron current densities and the responsivity can be obtained using Eq. (6).

Equations (10) and (11) show how the transit of carriers in each layer and the confinement at each heterointerface affect the current densities and, hence, the responsivity. An approximate but simplified relation may be obtained with certain assumptions. Assuming no recombination during transit except at the heterointerfaces, a simplified but approximate relation for responsivity $(\Re_0)$ may be obtained as

$$\Re_0 = \frac{q}{Mh\nu} \times \frac{(1-R_1)e^{-\alpha_{\mathrm{SiGe}}Md_w}}{(1 - 2\sqrt{R_1R_2}e^{-\alpha_{\mathrm{SiGe}}Md_w}\cos[2\beta L + \varphi_1 + \varphi_2] + R_1R_2e^{-2\alpha_{\mathrm{SiGe}}Md})} \times \sum_{i=1}^{M} \left[-\frac{(e^{\alpha_{\mathrm{SiGe}}d_w} - 1)}{\alpha_{\mathrm{SiGe}}d_w}\{e^{\alpha_{\mathrm{SiGe}}(M-r)d_w} - R_2e^{-\alpha_{\mathrm{SiGe}}(M-r+1)d_w}\} + (e^{\alpha_{\mathrm{SiGe}}d_w} - R_2e^{-\alpha_{\mathrm{SiGe}}d_w}) \right] f_h^r + \left[\frac{(e^{\alpha_{\mathrm{SiGe}}d_w} - 1)}{\alpha_{\mathrm{SiGe}}d_w}\{e^{\alpha_{\mathrm{SiGe}}(M-r)d_w} - R_2e^{-\alpha_{\mathrm{SiGe}}(M-r+1)d_w}\} - (1-R_2) \right] f_e^{M-r+1}, \tag{13}$$

which, in the limit $f_e, f_h \to 1$, converges to the expression for responsivity of a photodetector in the absence of any recombination.[10]

A spatial variation in optical field inside the cavity arises from the standing wave formed by the two counter propagating waves. For a very thin active layer, the power absorbed in the active region depends on its placement inside the cavity. This standing wave effect can be included by replacing α_{SiGe} with the effective absorption coefficient, $\alpha_{\mathrm{SiGe,eff}}$ (Ref. 10) in a simplified form as

$$\alpha_{\mathrm{SiGe,eff}} = \alpha_{\mathrm{SiGe}} \times \left(1 \pm \frac{\sin \beta d_w}{\beta d_w}\right), \tag{14}$$

where (+) or (−) sign corresponds to the maximum or minimum of the standing wave in the position of the active layer.

In case of multiple QW RCE photodetector, the layers (QWs) are distributed over a large thickness and the standing wave effect is not that significant as in a single QW RCE photodetector. However, any minor modification in the effective absorption coefficient in a multiple layer structure can be obtained taking the position average of optical field over the whole absorption region. An approximate expression for the effective absorption coefficient can be obtained as

$$\alpha_{\mathrm{SiGe,eff}} = \alpha_{\mathrm{SiGe}} \times \frac{\sum_{r=1}^{M}\left[1+\frac{\sin \beta d_w}{\beta d_w}\cos 2\beta\{(d_B+d_w)(M-r+1)-d_B-d_w/2+L_2\}\right]}{M}. \quad (15)$$

Depending on the cosine function on the right hand side of the above equation, the term within the bracket in the numerator may vary from $(1-\sin \beta d_w/\beta d_w)$ to $(1+\sin \beta d_w/\beta d_w)$. However, the averaging effect for large M may result in almost no change in α_{SiGe} caused by standing wave effect.

III. RESULTS AND DISCUSSIONS

The values of important material parameters required for calculation of responsivity are summarized in Table I for quick reference. The absorption coefficients (α_{SiGe}) are shown for well thickness (d_w) of 20 nm. Its value for other thicknesses can be derived following the discussion at the end of Sec. II B. Besides, doping concentrations of both P and N regions are taken to be 3×10^{24} m^{-3}, recombination rates for holes and electrons[15] are taken as $\sim10^9$ s^{-1}, the i layer is assumed to be purely intrinsic and the mirror reflectivities are taken as $R_1=0.49$ and $R_2=0.99$. For verification of the model, the sample structure and experimental data are taken from literature.[16] The sample structure is that of a RCE MQW photodetector with 20 (M) periods of alternate layers of Si and SiGe. The thicknesses of Si and SiGe alloy are 20 nm (d_B) and 9.3 nm (d_w), respectively, and the Ge-content (x) is 0.35. The responsivity at a fixed wavelength of 1.305 μm is computed using Eq. (6) and plotted as a function of reverse bias voltage in Fig. 3. A reasonably good agreement of the model is found with the experimental data given in the above reference.

Confinement of carriers and so, the responsivity depends on the band discontinuity at the heterointerfaces, which in turn depends on the Ge-content in the SiGe alloy. The responsivity of a RCE SiGe/Si MQW photodetector is plotted as a function of Ge-content for five different wavelengths (0.69, 0.85, 1.0, 1.3, and 1.55 μm) in Fig. 4. In Fig. 4(a), bias is taken to be 2 V. It can be seen from the figure that as the Ge-content increases, the responsivity decreases for $\lambda=0.69$ μm, initially increases and then decreases for $\lambda=0.85$ and 1.0 μm showing appearance of peak, and increases for $\lambda=1.3$ and $\lambda=1.55$ μm in the range of the Ge-content shown. The reasons for peaks may be given as follows. The initial rise in responsivity is due to the increase in absorption coefficient (α_{SiGe}) as Ge-content increases. However, if the Ge-content is made higher, the potential barrier at the heterointerface increases and, hence, the confinement also increases resulting in the loss of carriers due to recombination. Thus, the responsivity decreases after reaching a peak. Peaks may be seen for $\lambda=1.3$ and $\lambda=1.55$ μm also if Ge-content is increased further (>0.6). However, we have restricted our study for Ge-content <0.6 so that the analysis is valid for a practical Si/SiGe structure having tolerable strain due to lattice mismatch. The purpose of the present study is primarily to study the responsivity of the detector for long-haul communications. Our discussion will, henceforth, be focused only on these two wavelengths, i.e., 1.3 and 1.55 μm. The plot for a higher bias (8 V) is shown in Fig. 4(b). It can be seen that the responsivity is enhanced as the bias increases. The effect of bias on the responsivity is shown in detail in the next figure.

In Fig. 5(a), the responsivity of a RCE SiGe/Si MQW photodetector is plotted as a function of reverse bias for three different well-numbers (M) at 1.3 μm wavelength. It can be seen from the figure that the responsivity initially increases as the bias increases and finally becomes constant at a high bias. As the bias increases, the electric field increases, which reduces the effective potential barrier (e'_{vd}) at the heterointerface, thereby decreasing the confinement of carriers. Thus, the carrier loss by recombination at the heterointerface is reduced, and the responsivity increases with bias ultimately

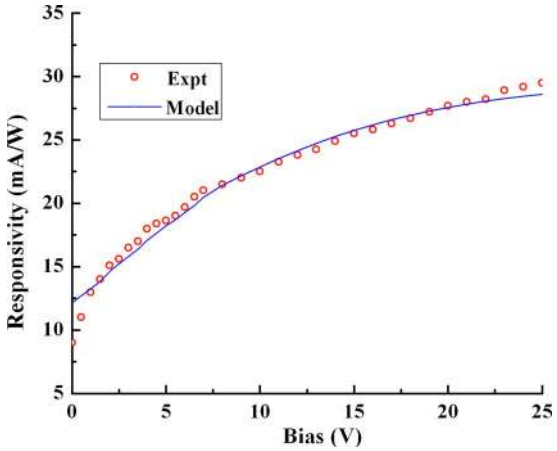

FIG. 3. (Color online) Responsivity vs reverse bias voltage plot for model verification. The experimental data taken from literature (Ref. 16) are shown by circles.

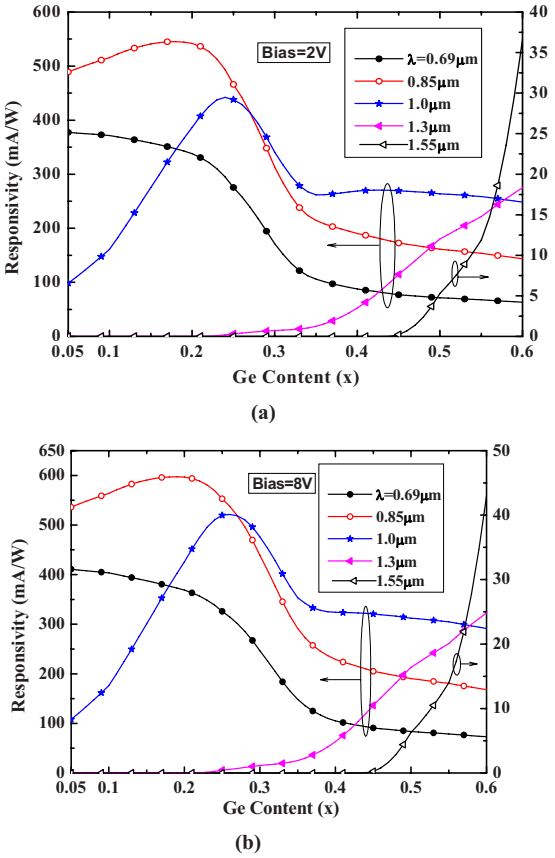

FIG. 4. (Color online) Responsivity of a RCE SiGe/Si MQW photodetector as a function of Ge-content (x), for five different values of λ (0.69, 0.85, 1.0, 1.3, and 1.55 μm), d_w=10 nm, d_B=20 nm, and number of wells (M)=30. In (a), bias=2 V and in (b), bias=8 V.

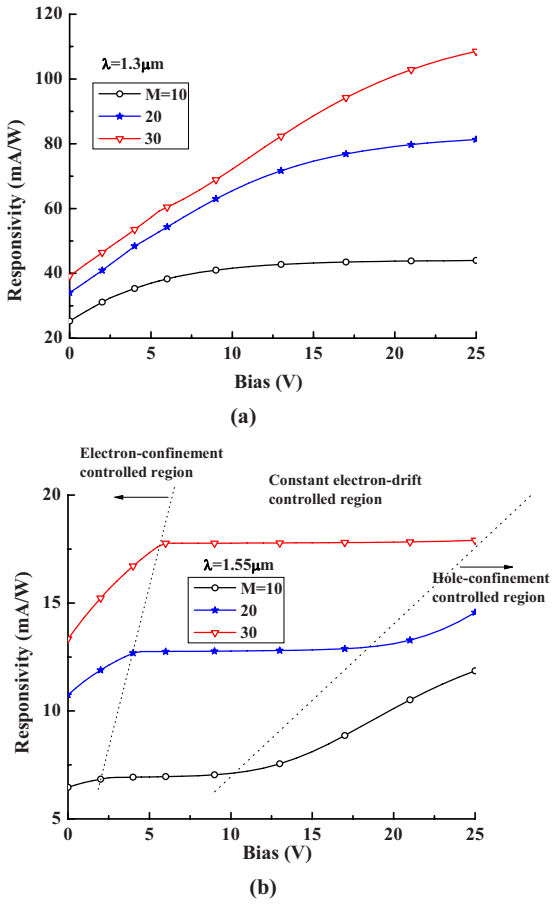

FIG. 5. (Color online) Responsivity of a RCE SiGe/Si MQW photodetector as a function of bias voltage with number of wells as parameter (M =10,20,30) keeping d_w fixed at 20 nm and d_B at 30 nm; (a) λ=1.3 μm, Ge-content 0.35 and (b) λ=1.55 μm, Ge-content 0.5.

reaching a constant value. The minimum bias at which the responsivity becomes constant is, however, more for larger M than that for smaller M. This is due to the increase in the loss of the confined carriers by recombination as explained next. First, for larger number of wells, the carriers have to travel more number of heterointerfaces and, so, there is more occurrence of confinement. Second, with the increase in the number of wells, the effective field at a heterointerface due to the applied bias decreases. So, the reduction of the effective potential barrier by the applied bias is now less thereby causing more confinement of the carriers at the heterointerface. Thus, higher bias is required with larger M for the responsivity to reach the constant value. Moreover, this constant responsivity is higher for larger number of wells (M) because of the increase in the total thickness for photoabsorption. In Fig. 5(b), the plot is shown for wavelength 1.55 μm. It is interesting to note here that for a certain range of bias (e.g., ~4–12 V for M=20), there is no significant change in responsivity. For the bias within that range or less, the loss of holes by recombination due to confinement is so high that there is no significant contribution of holes to the total current in the photodetector. The current is now predominantly controlled by the electrons moving without any confinement ($\Delta E_c \ll \Delta E_v$) in this bias range. However, for low enough bias, there may be confinement of electrons also and then, the responsivity decreases as the bias decreases. For high biases beyond plateau region, the responsivity increases with bias showing that the holes have started contributing to the total photocurrent because confinement of holes at the heterointerface reduces with the increase in the bias.

The variation of responsivity with well thickness d_w is shown in Fig. 6 for three different well-numbers (M =10,20,30) and for a fixed bias of 5 V. In Fig. 6(a), the plot is shown for the wavelength of 1.3 μm and in Fig. 6(b), it is shown for 1.55 μm. In general, the responsivity increases with the increase in the well thickness (d_w) because the increase in d_w results in the increased absorption and, hence, the increased responsivity. However, high d_w may reduce the bandwidth of the device through the increase in the transit time. It may be seen that the responsivity can be increased using large number of wells (M), but this benefit cannot be obtained after a high M when the carrier confinement at the heterointerfaces becomes significant thus reducing the bandwidth of the photodetector. For example, to give a relative estimate of the bandwidth as a function of well numbers, we use a crude approximation to see that while the bandwidth of the MQW photodetector with 10 wells is 6.8 GHz, that with 20 wells is 1.4 GHz and that with 30 wells is 0.7 GHz assuming thickness of each well as 50 nm. It may be mentioned here that true estimation of bandwidth may be obtained from the detailed analysis on the frequency response of this photodetector structure.

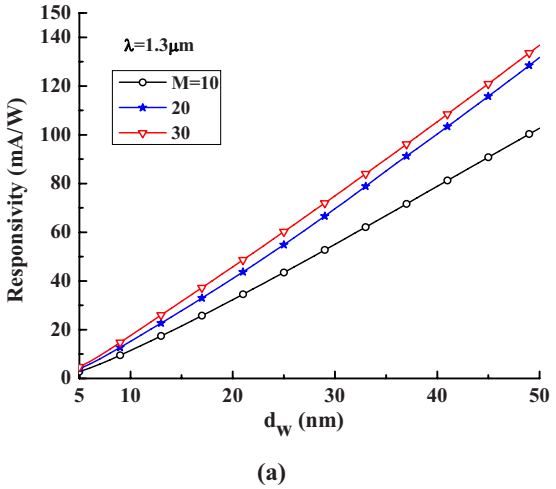

FIG. 6. (Color online) Variation of the responsivity of the photodetector as a function of well thickness (d_w) with M as parameter at a fixed bias of 5 V and d_B=100 nm. (a) λ=1.3 μm, Ge-content 0.35 and (b) λ=1.55 μm, Ge-content 0.5.

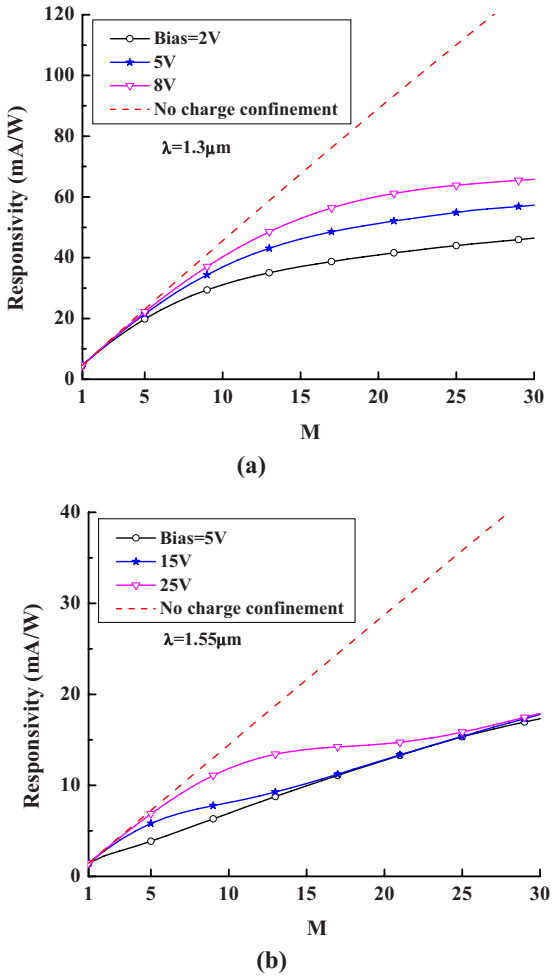

FIG. 7. (Color online) Dependence of responsivity on the number of wells for three different biases in a RCE SiGe/Si MQW photodetector taking d_w =20 nm and d_B=30 nm. (a) λ=1.3 μm, Ge-content 0.35 and (b) λ =1.55 μm, Ge-content 0.5.

The variation of responsivity of the photodetector with number of wells for three different biases at 1.3 μm is shown in Fig. 7(a). The responsivity increases with the increase in the number of wells; the rate of increment, however, decreases as the number of wells increases. In general, the responsivity increases with the number of wells mainly due to the increased absorption. However for larger number of wells, there are more heterointerfaces and, hence, the effect of confinement becomes significant causing loss of carriers as mentioned in an earlier paragraph. So, the rate of increment of the responsivity decreases as the number of wells increases. The dashed line shows the responsivity in the absence of confinement at the interface. It may be seen from the figure that the confinement can be reduced if the bias is increased (as mentioned before, Fig. 5). Similar plot for 1.55 μm wavelength is shown in Fig. 7(b). In this figure, Ge-content is kept fixed at a high value (0.5) to get appreciable responsivity at 1.55 μm. It can be seen that the effect of confinement in this case is highly significant even at a large bias. This is because of the large discontinuity in the valence band (ΔE_v) for high Ge-content. The variation of responsivity with M at large bias (25 V) is explained as follows. For small values of M, the linear increase (following dashed line) in the responsivity is due to the increased absorption. For large M (>5, for example), the carrier confinement at the heterointerface becomes significant. So, the increment in the responsivity gradually decreases with the increase in M (~5–20 region). As M increases further (>20), the confinement of holes becomes high, so a large number of holes are lost by recombination and there is negligible contribution of holes to the total photocurrent. This causes a drop in the responsivity, which is now mainly controlled by the electrons moving with constant velocity [constant electron drift region, Fig. 5(b)]. So, the responsivity becomes the same at all biases and increases due to the increase in the number of photogenerated electrons with M.

IV. CONCLUSION

The effect of Ge-content on the responsivity of a RCE SiGe/Si MQW photodetector has been investigated. The analysis has been done considering the effects of the applied bias and the subband positions in the well on the emission rate of the confined carriers from the potential trap at SiGe/Si heterointerfaces. The Ge-content dependent absorption coefficient and the recombination of the confined carriers at the heterointerfaces play important roles in the design of the

photodetector for high responsivity. It has been seen that by suitably controlling the Ge-content and well thickness, the responsivity can be enhanced. The responsivity can be increased by increasing the number of wells also, but the applied bias should be high enough to reduce the carrier confinement at the heterointerfaces. To obtain enhanced responsivity at low bias, structures having small number of wells with larger well thickness should be used.

ACKNOWLEDGMENTS

The authors wish to acknowledge the help of the colleagues in their research group in the department of Radio Physics and Electronics, University of Calcutta. Useful suggestions from reviewers are also thankfully acknowledged.

[1]P. Bhattacharya, *Semiconductor Optoelectronic Devices* (Prentice-Hall of India Pvt. Ltd, New Delhi, 2002).
[2]N. R. Das, Y. M. Batawy, and M. J. Deen, in *Integrated Optoelectronics*, edited by M. J. Deen, D. Misra, and M. Ruzylo, (ECS, NJ, (2002) PV 2002–4, 163.
[3]L. Colace, M. Balbi, G. Masini, and G. Assanto, Appl. Phys. Lett. **88**, 101111 (2006).
[4]U. Dümler, M. Möller, A. Bielik, T. Ellermeyer, H. Langenhagen, W. Walthes, and J. Mejri, Electron. Lett. **42**, 21 (2006).
[5]J. Sturm, M. Leifhelm, H. Schatzmayr, S. Groiss, and H. Zimmermann, IEEE J. Solid-State Circuits **40**, 1406 (2005).
[6]M. Salib, L. Liao, R. Jones, M. Morse, A. Liu, D. Samara-Rubio, D. Alduino, and M. Paniccia, Intel Technol. J. **8**, 143 (2004).
[7]S. M. Csutak, J. D. Schaub, B. Yang, and J. C. Campbell, Proc. SPIE **4997**, 135, (2003).
[8]S. Koh, K. Sawano, and Y. Shiraki, 1st IEEE International Conference on Group IV Photonics, 2004 (unpublished) p. 61.
[9]S. C. Jain, *Germanium-Silicon Strained Layers and Heterostructures* (Academic Press, Boston, 1994).
[10]M. S. Ünlü and S. Strite, J. Appl. Phys. **78**, 607 (1995).
[11]J. E. Roth, O. Fidaner, R. K. Schaevitz, Y.-H. Kuo, T. I. Kamins, J. S. Harris, Jr., and D. A. B. Miller, Opt. Express **15**, 5851 (2007).
[12]R. Braunstein, A. R. Moore, and F. Herman, Phys. Rev. **109**, 695 (1958).
[13]R. People, IEEE J. Quantum Electron. **22**, 1696 (1986).
[14]N. R. Das and M. J. Deen, IEEE J. Quantum Electron. **37**, 1574 (2001).
[15]E. Gaubas, R. Tomašiunas, G. Eneman, R. Delhougne, and E. Simone, Semicond. Sci. Technol. **20**, 1052 (2005).
[16]C. Li, Q. Yang, H. Wang, J. Yu, Q. Wang, Y. Li, J. Zhou, H. Huang, and X. Ren, IEEE Photon. Technol. Lett. **12**, 1373 (2000).